JEE Journal of Ecological Engineering

Journal of Ecological Engineering, 2026, 27(5), 179–199
https://doi.org/10.12911/22998993/216243
ISSN 2299–8993, License CC-BY 4.0

Received: 2025.10.02
Accepted: 2026.03.16
Published: 2026.04.01

Assessment of soil fertility variability for maize production in highland agroecosystems of Peru

Erika Garcia[1], Dennis Ccopi[1], Edilson Requena-Rojas[1], Samuel Sanabria-Quispe[1], Alberto Arias-Arredondo[1], Esthefany Gavino[1], Andres Azabache[2], Samuel Pizarro[1*]

[1] Estación Experimental Agraria Santa Ana, Dirección De Servicios Estratégicos Agrarios, Instituto Nacional de Innovación Agraria (INIA), Carretera Saños Grande – Hualahoyo Km 8 Santa Ana, Huancayo, Junín 12006, Peru
[2] Universidad Nacional del Centro del Perú, Facultad de agronomía, Huancayo, Junín 12006, Peru
* Corresponding author's e-mail: samuel.pizarro@untrm.edu.pe

ABSTRACT

Maize (*Zea mays* L.) is central to food, feed, and rural livelihoods, yet the yields in Peru's highlands remain modest, underscoring the need for spatially explicit soil diagnostics. This study aimed to characterize the spatial variability of soil fertility in a highland maize production area of the southern Mantaro Valley and translate those patterns into site-specific management zones. The authors sampled the arable layer (0–30 cm) at 100 plots and analyzed pH, electrical conductivity, exchangeable acidity, texture, organic matter (OM), total nitrogen (N), available phosphorus (P), available potassium (K), exchangeable cations (Ca, Mg, Na, K), and calcium carbonate ($CaCO_3$). Laboratory data were integrated with environmental covariates using geostatistics, Random Forest, and GIS to generate high-resolution maps. Results showed uneven distributions in key attributes about 25% of the area with P deficiency, 15% with localized K shortages, and ~20% with OM < 2% while pH and CEC were comparatively stable. Random Forest achieved strong predictive performance for relatively stable properties (e.g., OM, pH, exchangeable cations), whereas mobile nutrients (available P, exchangeable K) were less predictable. The resulting products constitute the first high-resolution soil-fertility baseline for maize in the southern Mantaro Valley. The maps delineate fertilization management zones and provide a practical basis for preliminary rate recommendations that target constraints while avoiding surpluses. Future work will refine these zoned recommendations through yield-response trials, seasonal monitoring of mobile nutrients, and farmer-centered decision-support tools, with the goal of improving nutrient-use efficiency, sustaining maize productivity, and reducing environmental risks across the valley.

Keywords: spatial variability, random forest, site-specific management, Maize (*Zea mays* L.), soil fertility mapping

INTRODUCTION

Maize (*Zea mays* L.) is one of the most important crops worldwide due to its high yield potential, diverse uses, and broad distribution. It plays a key role in human nutrition, livestock feed production, and serves as a raw material for various industries (FAO., 2003; Wang et al., 2024). Currently, it is cereal with the highest production volume globally and is projected to become the most widely planted and traded crop in the coming decade (Tikuye and Ray, 2025). In developing countries, the significance of maize is particularly evident, accounting for more than 20% of the population's caloric intake (Wang et al., 2024).

Maize has high soil requirements and shows notable sensitivity to low fertility conditions (Dawar et al., 2022). In Peruvian highland agroecosystems, where floury maize yields average only around 2.5 t/ha approximately three times lower than dent or semident varieties under more favorable conditions (Zambrano et al., 2021), this sensitivity to soil constraints is particularly evident. Several studies have demonstrated that growth and yield are significantly affected when the crop is grown in the soils with low organic

matter content and limited availability of essential nutrients (Abrol et al., 2024; Dawar et al., 2022). To reach its maximum productive potential, maize requires the soils with adequate physical, chemical, and biological characteristics, including appropriate texture and structure, pH, macro and micronutrients, available moisture, and organic matter (Kuunya et al., 2025). The crop performs best in loam-textured soils that are well-drained with good water retention capacity, and a slightly acidic to neutral pH between 6.0 and 7.5, which optimizes phosphorus availability – one of the key nutrients for its development (MacCarthy et al., 2023). In highland agroecosystems, these ideal conditions are often compromised by shallow soils, natural acidity, low organic matter accumulation due to cooler temperatures, as well as nutrient depletion from continuous cultivation and erosion processes (Zambrano et al., 2021).

Soil chemical properties are fundamental determinants of nutrient availability and crop performance. Soil pH regulates nutrient accessibility; when it drops below 5.5, aluminum and manganese toxicity can increase, damaging roots and hindering the uptake of nitrogen, phosphorus, calcium, and magnesium (Nwite et al., 2022; Rao et al., 2019). Cation exchange capacity (CEC) enables soil to retain essential nutrients such as Ca^{2+}, Mg^{2+}, and K^{+}, which are crucial for plant nutrition (Al-Shammary et al., 2024; Zhou et al., 2024). Electrical conductivity (EC) reflects dissolved salt levels; elevated EC causes root stress that limits water uptake and stunts growth (Al-Shammary et al., 2024). Furthermore, nitrogen supports vegetative growth, phosphorus promotes root and reproductive development, and potassium enhances grain quality and resistance to pests, drought, and diseases (Shahid et al., 2023). In calcareous soils with high calcium carbonate ($CaCO_3$) content, phosphorus can become fixed, reducing its availability to plants (Igwe and Nkemakosi, 2007).

Physical soil properties are equally critical for maize cultivation. Soil texture the proportion of sand, silt, and clay directly affects water and nutrient retention, with loamy soils providing the ideal balance for crops like maize (Li et al., 2022). Organic matter improves soil structure, enhances water retention, and stimulates microbial activity, which helps release nutrients, such as nitrogen, phosphorus, and potassium (Julca-Otiniano et al., 2006). However, these properties are not static; they change over time due to agricultural practices, erosion, irrigation, and fertilization, leading to considerable spatial variability within the same field. This variability directly impacts soil fertility patterns and crop yield potential, particularly in topographically complex highland environments where erosion and deposition processes create pronounced fertility gradients.

Understanding and managing spatial variability in soil fertility is essential for optimizing agricultural productivity and resource use efficiency. This variability refers to differences in soil properties within the same field that affect crop growth and fertilizer effectiveness (Ingle et al., 2018). In highland agroecosystems, factors such as slope position, water flow patterns, historical land use, and erosion intensity contribute to highly heterogeneous soil conditions. Consequently, uniform management practices applying the same fertilizer rates across entire fields often lead to nutrient imbalances, with some areas receiving insufficient nutrients while others experience excess applications that increase production costs and environmental risks. Adapting agricultural practices based on site-specific soil information is therefore essential for improving crop performance and sustainability (Tamburi et al., 2021).

Site-specific fertilization recommendations based on soil fertility mapping have demonstrated significant benefits across diverse agricultural systems worldwide. In Europe, adjusting phosphorus doses to target fertility classes has prevented excessive accumulation and reduced runoff losses (Steinfurth et al., 2022). In Asia, establishing critical soil values for nitrogen, phosphorus, and potassium enabled fertilizer reductions of 17–43% without compromising productivity (Yang et al., 2024), In turn, nitrogen fertilization in spring maize achieved optimal yields with split applications of approximately 180 kg/ha (Jia et al., 2023). In Africa, site-specific nitrogen recommendations increased nitrogen use efficiency by 30% and significantly improved wheat yields compared to blanket fertilizer applications (Liben et al., 2024). Similarly, nutrient offtake models in perennial crops, such as cocoa, have shown greater profitability compared with uniform application schemes (Vasquez-Zambrano et al., 2025). This evidence demonstrates that well-founded fertilization recommendations not only enhance agricultural productivity, but also promote more sustainable soil resource management. However, such approaches remain underutilized in Peruvian highland agriculture, where smallholder farmers

typically rely on generalized recommendations that do not account for local soil variability.

Effective implementation of site-specific nutrient management requires accurate characterization and mapping of soil fertility patterns. Traditionally, geostatistical techniques such as ordinary kriging (OK) have been used to predict spatial distribution of soil variables including pH, organic matter, phosphorus, and potassium (Ismaili and Moughli, 2014; Valera and Rodríguez, 2023). OK relies on spatial autocorrelation to interpolate values based on neighboring observations, effectively capturing regional trends, but often failing to resolve fine-scale variability critical for micro-parcel management. This limitation is particularly problematic in smallholder systems where plot sizes are small and management histories are highly variable, resulting in abrupt spatial transitions that autocorrelation-based methods cannot adequately represent. In contrast, machine learning algorithms, such as random forest (RF), have gained prominence due to their capacity to model non-linear relationships, integrate multiple environmental covariates, and capture complex spatial patterns at fine resolution. Recent studies demonstrate that RF outperforms conventional geostatistical methods in spatial prediction of soil properties and fertility mapping, particularly for micro-scale assessments (Dharumarajan et al., 2017; Shahare et al., 2024). The integration of RF with geographic information systems (GIS) represents a promising approach for delineating site-specific management zones in fragmented agricultural landscapes, improving fertilizer use efficiency, and promoting more sustainable agricultural practices (Urso et al., 2023).

Despite the recognized importance of spatial soil fertility assessment, comprehensive studies characterizing the soil variability in Peruvian highland maize production systems remain limited. Most existing fertilization recommendations for the region are based on generalized guidelines that do not reflect local soil conditions or account for within-field variability, potentially limiting both productivity and resource use efficiency. This knowledge gap is particularly critical given the economic importance of maize for highland farmers and the environmental sensitivity of these agroecosystems to inappropriate nutrient management.

The main objective of this study was to characterize the spatial variability of soil fertility properties in a highland maize production area of Peru. Specifically, key properties of the arable layer were evaluated, including pH, electrical conductivity, exchangeable acidity, texture, organic matter, total nitrogen, available phosphorus, available potassium, exchangeable cations, and calcium carbonate. Using geostatistical techniques, machine learning algorithms (random forest), and GIS tools, the spatial distribution of these properties were mapped to identify fertility patterns and develop site-specific management zones. The findings will provide a foundation for tailored fertilization recommendations that can enhance maize productivity while promoting more efficient and sustainable use of soil resources in highland agroecosystems.

MATERIALS AND METHODS

Study area

The study was conducted in Huayucachi district, Huancayo province, Junín region, Peru (12°08′ S, 75°13′ W, 3.300 masl), located in the Mantaro River Valley, a major agricultural area in the central Peruvian highlands (MIDAGRI, 2009) (Figure 1). The climate is temperate subhumid with mean annual temperatures of 12–15 °C and precipitation concentrated between November and April, necessitating supplementary irrigation during the dry season (May–October) (Senamhi, 2020).

Agriculture is the predominant economic activity, characterized by smallholder farming systems with fragmented landholdings. The main crops include maize (*Zea mays* L.), potato (*Solanum tuberosum* L.), faba bean (*Vicia faba* L.), pea (*Pisum sativum* L.) and barley (*Hordeum vulgare* L.). Soils exhibit considerable spatial variability resulting from continuous cultivation, differential fertilizer application, erosion on sloped terrain, and inadequate nutrient replenishment, creating a highly heterogeneous fertility landscape that impacts crop productivity (Garay and Ochoa, 2010).

Soil sample collection

A total of 100 composite soil samples were collected in July 2024 from the topsoil layer (0–30 cm depth), following the standard protocol recommended by FAO for soil fertility assessment and nutrient monitoring (FAO., 2006,

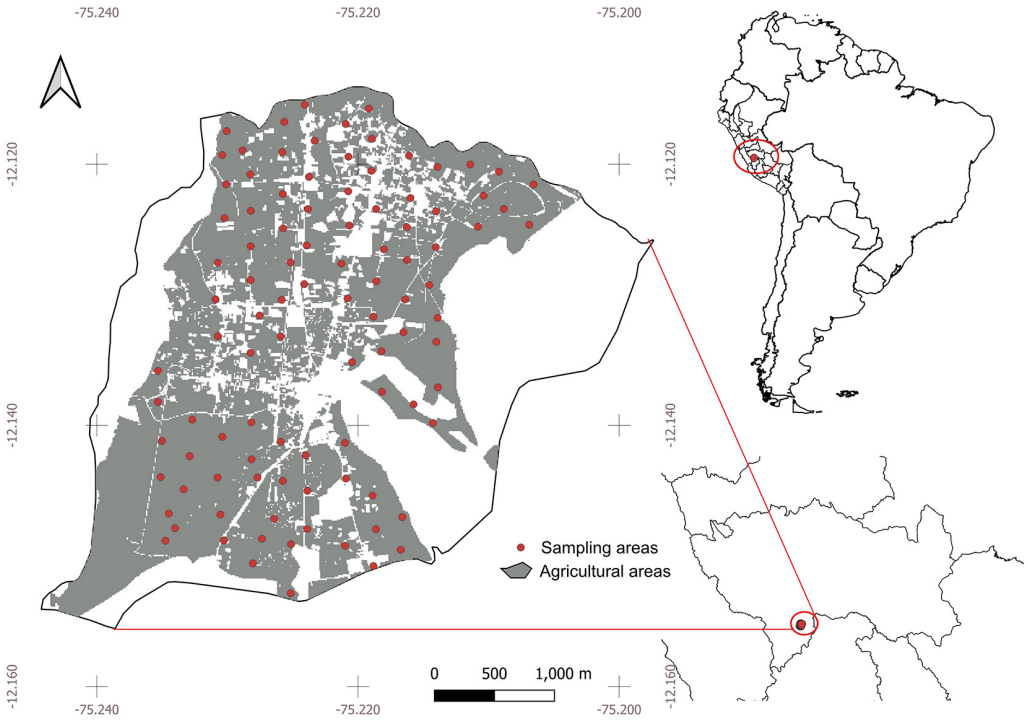

Figure 1. Location map of the study area

2017). Sampling locations were determined using a regular hexagonal grid designed in QGIS and loaded into the QField mobile application for field navigation. The grid was slightly modified in the field when sampling points fell on rural buildings or non-agricultural areas, with these points relocated to the nearest agricultural parcel to maintain representative spatial coverage.

One composite sample was collected per agricultural plot, with each composite consisting of nine subsamples arranged in a systematic grid pattern within the plot. Each sampling location was georeferenced using QField on a mobile device with integrated GPS, and the subsamples were thoroughly homogenized in the field to obtain approximately 1 kg of representative soil per composite sample. This composite sampling approach minimizes within-plot spatial variability and provides an adequate representation of soil properties in relatively homogeneous sampling units (FAO., 2006, 2017).

Laboratory analysis methods

The soil samples were air-dried at room temperature, disaggregated, and sieved (2 mm) prior to analysis at the soil, water, and foliar laboratory of INIA Santa Ana Experimental Station, Huancayo, Peru. Soil pH and electrical conductivity (EC) were measured in 1:1 soil-water suspension and saturation extract, respectively, following US EPA Method 9045D (US EPA, 2004) and ISO 11265:1994 (ISO, 1996). Texture was determined by the Bouyoucos hydrometer method. Organic matter (OM) was analyzed by Walkley-Black digestion, with total nitrogen (N) estimated as 5% of OM. Available phosphorus (P) was extracted using the Olsen method (0.5 M $NaHCO_3$) and quantified colorimetrically. Available potassium (K) and exchangeable cations (Ca^{2+}, Mg^{2+}, Na^{+}, Al^{3+}) were determined by optical emission spectrometry after ammonium acetate extraction; the sum of basic cations represents effective cation exchange capacity (CEC). Calcium carbonate equivalent ($CaCO_3$) was determined by acid neutralization. All methods followed SEMARNAT (2002) unless otherwise specified (ISO, 1994; NOM-021-RECNAT-2000, 2002; UEPA, 2004).

Covariate analysis

To model the spatial variability of soil properties, environmental covariates derived from remote sensing, topographic factors, and distance variables were integrated. Multispectral reflectance from Sentinel-2 and derived spectral indices (NDVI, EVI, MSAVI, GCVI, NDWI, among others) have proven to be relevant predictors of

soil properties, such as pH, organic matter, and salinity (Abdullah et al., 2025; Dharumarajan et al., 2017; Urbina-Salazar et al., 2023). Spectral transformations, such as Tasseled Cap components and topographic attributes (elevation, slope, aspect) also contribute significantly to explaining soil variability (Mirzaeitalarposhti et al., 2022a; Phinzi et al., 2025). Likewise, Sentinel-1 radar information (VV/VH backscatter and GLCM texture metrics) has been successfully used in the mapping of salinity and other soil properties (Ma et al., 2021; Tola et al., 2024). Finally, distance variables to rivers and roads have been employed as proxies of hydro-geomorphic controls and anthropogenic pressure in different agricultural contexts (Phinzi et al., 2025; Urbina-Salazar et al., 2023) (Table 1).

Machine learning model

The RF algorithm was used to predict the soil properties related to fertility and texture. This approach combines multiple decision trees trained on bootstrap samples and randomly selects predictors at each split, integrating the results through averaging (Bhanukiran Reddy et al., 2024; Bravo-García et al., 2025). The model was trained with an 80/20 train–test split, stratified on the response variable, and evaluated using 5-fold cross-validation. For hyperparameter tuning, different configurations were explored for the number of predictors sampled at each split (mtry = 5–27), the minimum node size (min.node.size = 5), the sample fraction (sample.fraction = 0.1–1.0, step 0.1), and the number of trees (num.trees = 50–1000, step 50) (Pizarro et al., 2025). The optimal model was selected based on the lowest root mean square error (RMSE) in cross-validation. The final performance on the test set was evaluated using the coefficient of determination (R^2), RMSE, mean absolute error (MAE), and the ratio of performance to deviation (RPD = σy / RMSE). Predictor variables consisted of the previously described environmental and remote sensing covariates, after correlation filtering to reduce multicollinearity (Chai and Draxler, 2014). In addition, variable importance profiles facilitated the identification of dominant drivers and provided insights useful for guiding site-specific soil management decisions (Mouazen and Shi, 2021).

Table 1. Environmental covariates used in modeling

Group	Covariates (variable names)	Description and function	Key references
Multispectral reflectance	blue, green, red, re1, re2, re3, nir, nir2, waterVapor, swir1, swir2	Sentinel-2 spectral bands in the visible, red-edge, near-infrared (NIR B8 & narrow NIR B8A), water vapor, and shortwave infrared (SWIR). These bands capture soil color, mineral composition, vegetation cover, and surface moisture conditions.	(Abdullah et al., 2025; Dharumarajan et al., 2017)
Spectral indices	NDVI, MSAVI, EVI, GCVI, NDWI, NDWI2, MODCRC, NDTI, NBRI, TVI, MTCI, STI, ARVI	Vegetation, chlorophyll, water, soil, and disturbance indicators derived from spectral data, summarizing canopy vigor, greenness, water status, and surface stress.	(Phinzi et al., 2025; Urbina-Salazar et al., 2023)
Spectral transforms	brightness, greenness, wetness	Tasseled Cap components representing gradients of soil brightness, canopy greenness, and surface or soil wetness.	(Crist and Cicone, 1984; Mirzaeitalarposhti et al., 2022a)
Topography	elevation, slope, aspect	Terrain attributes derived from DEMs that regulate energy balance, water redistribution, erosion, deposition, and local microclimate.	(Phinzi et al., 2025)
SAR backscatter & ratios	VV_a, VH_a, VV_d, VH_d, ratio_VH_VV_a, ratio_VH_VV_d	Sentinel-1 C-band backscatter in ascending/descending passes and VH/VV ratios, sensitive to surface roughness, structural properties, and soil moisture, independent of cloud cover.	(Ma et al., 2021; Tola et al., 2024)
SAR texture & statistics	VH_d_sd, VV_d_sd, VH_d_25, VH_d_75, VV_d_25, VV_d_75, VH_d_idm, VH_d_contrast, VH_d_corr, VH_d_var, VH_d_ent, VH_d_svar, VH_d_sent, VH_d_asm	Statistical descriptors (standard deviation, quantiles) and GLCM texture metrics (inverse difference moment, contrast, correlation, variance, entropy, angular second moment, etc.) used to characterize spatial structure and heterogeneity.	(Haralick et al., 1973; Tola et al., 2024)
Distance factors	D_rivers, D_Mroads, D_mroads	Euclidean distance to rivers, major and minor roads, serving as proxies for hydro-geomorphic processes and human disturbance.	(McBratney et al., 2003; Urbina-Salazar et al., 2023)

Soil suitability classification criteria for maize production

Table 2 shows the soil fertility thresholds for maize cultivation, established from INIA technical manuals (2014; 2017) and specialized literature (Havlin et al., 2014). Key parameters include pH, organic matter, nitrogen, phosphorus, potassium, CEC, calcium carbonate, electrical conductivity, and texture. Optimal ranges, such as pH 5.5–7.5, organic matter >2%, and phosphorus >11 ppm, promote nutrient availability and crop yield, while loam textures and electrical conductivity <200 mS/m optimize water balance and reduce salinity risks. These values classify soil fertility as low, medium, or high, serving as a guide for soil diagnosis and maize management.

Fertilizer demand

The fertilization demand of maize (*Zea mays* L.) was estimated based on the nutrient requirements per ton of grain yield reported in the literature (FAO, 2006b), corresponding to nitrogen (N = 22 kg t^{-1}), phosphorus (P = 4 kg t^{-1}), potassium (K = 19 kg t^{-1}), calcium (Ca = 3 kg t^{-1}), and magnesium (Mg = 3 kg t^{-1}). These values were multiplied by the target yield (2.5 t ha^{-1}) to obtain the total elemental nutrient demand (Zambrano et al., 2021). Subsequently, the results were converted into fertilizer form using specific conversion factors (FC), namely N = 1.00, P = 2.29 (to P_2O_5), K = 1.21 (to K_2O), Ca = 1.40 (to CaO) and Mg = 1.66 (to MgO). In this manner, the estimated demand for a yield of 2.5 t ha^{-1} was 55.0 kg N ha^{-1}, 22.9 kg P_2O_5 ha^{-1}, 57.5 kg K_2O ha^{-1}, 10.5 kg CaO ha^{-1} and 12.5 kg MgO ha^{-1}.

Estimation of soil nutrient supply into fertilizer-equivalent units

The contribution of the soil to nutrient supply was quantified from laboratory analyses of the samples collected at 0–25 cm depth, integrating soil bulk density estimation, nutrient conversion, and correction factors for nutrient availability.

Bulk density (BD, t m^{-3}) was estimated using a pedotransfer function (PTF) that relates BD to soil texture and organic matter content (Manrique and Jones, 1991; Rawls et al., 2004) Equation 1:

$$BD = 1.66 - 0.004 \times clay - \\ - 0.002 \times silt - 0.005 \times OM \quad (1)$$

Where clay and silt are expressed as percentages of particle size fractions, and OM is the soil organic matter content (%). The predicted BD values were constrained between 0.9 and 1.7 t m^{-3}, a realistic range for mineral soils (Bernoux et al., 1998). The resulting BD was used to compute soil mass per hectare for the sampled depth Equation 2:

$$Soil\ mass\ (kg\ ha^{-1}) = BD \times \\ \times depth\ (m) \times 10{,}000 \times 1000 \quad (2)$$

For conversion of elements the nutrients reported in ppm (mg kg^{-1}) were converted to kg ha^{-1} using Equation 3:

$$kg\ ha^{-1} = ppm \times BD \times depth\ (m) \quad (3)$$

Table 2. Soil chemical suitability classes for amylaceous maize based on laboratory thresholds

Parameter	Low / Limiting	Medium/Acceptable	High/Suitable	References
Organic matter (OM, %)	< 2.0	2.0–4.0	> 4.0	(Alvarado and Chavez, 2009; MIDAGRI, 2020)
Total nitrogen (N, %)	< 0.10	0.10–0.20	> 0.20	(CIMMYT, 1988)
Available phosphorus (P, ppm, Olsen)	< 10	10–15	> 15	(CIMMYT, 1988; INIA, 2008)
Available potassium (K, ppm)	< 100	100–150	> 150	(Alvarado and Chavez, 2009; CIMMYT, 1988)
Effective CEC (cmol/kg)	< 10	10–20	> 20	(NOM-021-RECNAT-2000, 2002)
Calcium carbonate ($CaCO_3$, %)	> 20 (Excessive, limiting)	10–20 (Moderate, caution)	< 10 (Suitable)	(FAO, 2006; MIDAGRI, 2020; Saidi, 2012)
Electrical conductivity (EC, mS/m)	> 400 (Saline)	200 – 400 (Slightly saline)	< 200 (Non-saline)	(FAO, 1976, 2006)
pH (water 1:2.5)	< 5.5 or > 7.5 (Limiting)	5.5 – 6.0 or 7.0 – 7.5 (Acceptable)	6.0 – 7.0 (Optimal)	(FAO, 2006)
Texture	Very clayey / very sandy (limiting)	Clay loam (acceptable)	Loam (suitable)	FAO (1976); (MIDAGRI, 2019, 2020)

Cations expressed in cmol(+) kg^{-1} were first converted to mg kg^{-1} using atomic weight and valence, then to kg ha^{-1} with the same factor (Burt, 2004).

Potential nitrogen supply was estimated from soil organic matter content, assuming 5% N within OM and a mineralization coefficient of 1.3% during the cropping cycle. To reflect the actual duration of the crop in the field, a seasonal scaling factor equal to the ratio of months under cultivation to 12 months was applied (Raun and Johnson, 1999; Smil, 1999) Equation 4.

$$N_{mineralized} = Soil\ mass \times \frac{\%OM}{100} \times \frac{N_{OM}}{100} \times \times \frac{Mineralization}{100} \times Season\ fraction \quad (4)$$

No recovery fraction was applied at this stage, since recovery is accounted for later in the fertilization efficiency step.

Availability corrections

Since not all nutrients measured in the soil are available to crops, correction factors (FD) were applied for P and K.

The available elemental nutrient supply was transformed into fertilizer-equivalent units using molecular weight conversion factors: N = 1.00, P = 2.29 (P_2O_5), K = 1.21 (K_2O), Ca = 1.40 (CaO), Mg = 1.66 (MgO), and S = 1.00 (FAO, 2006).

Net nutrient requirement and fertilizer dose

The net nutrient requirement was defined as the difference between the crop demand and the soil nutrient supply for each nutrient, both expressed in fertilizer-equivalent form. To avoid negative values, which would imply an excess supply from the soil, the calculation was constrained to a minimum of zero:

$$\mathrm{NetReq}_i^F = max(0, \mathrm{Demand}_i^F - \mathrm{Supply}_i^F) \quad (5)$$

where: Demand_i^F is the crop demand in fertilizer form (kg ha^{-1}), and Supply_i^F is the soil contribution in fertilizer form (kg ha^{-1}). Thus, if the soil nutrient supply exceeds the crop demand, no additional fertilizer is required (NetReq_i^F = 0) (Capetillo-Burela et al., 2021).

The required fertilizer dose was then estimated by correcting the net requirement with a nutrient-specific fertilizer use efficiency factor (FE_i) which accounts for the fraction of applied fertilizer actually taken up by the crop (Rangaiah et al., 2024) (Table 3):

$$Dose_i^F = \frac{NetReq_i^F}{FE_i} \quad (6)$$

Finally, an empirical adjustment factor Co=1.55 was applied to the calculated fertilizer dose. This factor originates from local calibration designed to adjust the calculated dose to the crop performance observed under field conditions. While there is no published precedent for this specific value in the maize literature, similar empirical correction factors are commonly used in agronomic calibration when site-specific uptake dynamics deviate from general models (LIU et al., 2012; Maiti et al., 2006) (Table 4, 5).

Table 3. Correction factors (FD) for phosphorus availability according to soil pH (Mcfarland et al., 2001)

Soil pH	FD (fraction of total P available)
≤ 4.5	0.08
4.6–5.0	0.10
5.1–6.0	0.15
6.1–7.0	0.30
> 7.0	0.15

Table 4. Correction factors (FD) for potassium availability according to cation exchange capacity, CEC (Dobermann, 2001)

CEC (cmol(+) kg^{-1})	FD (fraction of total K available)
< 10	0.50
10–14.9	0.35
15–19.9	0.25
≥ 20	0.15

Statistical analysis and geospatial tools

Statistical analyses were conducted in R software version 4.4.0 (R Core Team, 2024), employing a range of specialized packages. Data visualization was carried out with ggplot2 and plotly (Wickham et al., 2019), while spatial data handling and analysis relied on sf, sp, raster, and terra (Pebesma, 2018). Machine learning modeling was performed with the randomForest package (Liaw and Wiener, 2002), used for predicting soil properties and assessing variable importance.

Table 5. Fertilizer efficiency factors (FE) used for nutrient dose calculations

Nutrient	Fertilizer efficiency (FE, fraction)	References
N	0.20	(Randhawa et al., 2021)
P	0.20	(Fageria and Baligar, 2014)
K	0.40	(Yermiyahu et al., 2017)
Ca	0.40	(Butphu et al., 2020)

In addition, Google Earth Engine (GEE) was employed for large-scale preprocessing of Sentinel-2 imagery, spectral index computation, and data extraction (Gorelick et al., 2017). Finally, QGIS software (QGIS Development Team, 2024) was applied for cartographic editing, plot georeferencing, and visual validation of results.

RESULTS

Descriptive analysis of soil fertility parameters

Table 6 shows the descriptive statistics of the main soil fertility parameters evaluated across 100 agricultural plots in the study area. The results reveal a high degree of spatial variability in several key indicators relevant to maize production. Among the exchangeable cations, calcium (Ca^{2+}) showed the highest average concentration (24.29 cmol·kg^{-1}), with moderate variability (CV = 64.07%). In contrast, magnesium (Mg^{2+}), sodium (Na^{+}), and potassium (K^{+}) exhibited much higher coefficients of variation (79.84–92.65%), indicating marked heterogeneity in nutrient availability among plots. The effective CEC averaged 26.51 cmol·kg^{-1}, suggesting a generally good nutrient retention capacity.

The calcium carbonate content ($CaCO_3$) was also highly variable (CV = 74.88%), with values ranging from 0 to 20.2%, which can influence nutrient availability and soil pH buffering. EC values indicated low to moderate salinity levels, with a mean of 0.68 dS·m^{-1} and moderate variability (CV = 36.02%). In terms of macronutrients, both available phosphorus (P) and available potassium (K) displayed high variability (CV > 70%), with maximum values of 88.48 ppm and 835.64 ppm, respectively. These findings highlight the need for site-specific fertilization strategies to optimize maize yield. Organic matter (OM) content (mean = 3.75%) and total nitrogen (N) (mean = 0.19%) also showed high variability (CV ≈ 63%), which can significantly influence soil fertility and crop development.

Soil pH was relatively homogeneous (CV = 3.51%), with a slightly alkaline average of 7.75, which is suitable for maize cultivation. Regarding soil texture, results indicate a predominance of sandy loam, with mean contents of sand (43.42%), silt (33.58%), and clay (23.00%). These proportions, together with the low variability of texture

Table 6. Descriptive analysis of soil fertility parameters

Variable	Mean ± SD	CV (%)	Min	Max	Skewness (As)	Kurtosis (Kr)
Exchangeable Ca^{2+} (cmol·kg^{-1})	24.29±15.56	64.07	2.23	50.83	0.11	-1.47
Exchangeable Mg^{2+} (cmol·kg^{-1})	1.73±1.38	79.84	0.20	7.46	1.72	4.23
Exchangeable Na^{+} (cmol·kg^{-1})	0.14± 0.13	92.39	0.02	0.92	3.34	15.96
Exchangeable K^{+} (cmol·kg^{-1})	0.35 ± 0.32	92.65	0.04	2.46	3.37	17.24
Effective CEC (cmol·kg^{-1})	26.51 ± 15.63	58.96	2.50	61.00	0.90	3.00
$CaCO_3$ (%)	10.04 ± 7.52	74.88	0.00	20.20	0.10	-1.65
EC (dS·m^{-1})	0.68 ± 0.25	36.02	2.35	19.23	2.01	7.59
Available P (ppm)	17.56 ± 16.44	93.61	2.45	88.48	2.21	5.29
Available K (ppm)	179 ± 127	70.84	37.55	835.64	3.38	13.63
pH	7.75 ± 0.27	3.51	6.10	8.10	-2.62	12.19
Organic matter (OM, %)	3.75 ± 2.35	62.60	0.73	17.32	2.46	9.84
Total, nitrogen (N, %)	0.19 ± 0.12	62.62	0.04	0.87	2.46	9.82
Sand (%)	43.42±11.11	25.59	17.22	74.10	0.05	-0.20
Silt (%)	33.58 ± 7.89	23.51	16.98	53.93	0.51	-0.21
Clay (%)	23.00 ± 7.62	33.11	4.86	53.07	0.57	1.64

components, suggest moderate physical limitations for root development and water retention.

Prediction parameters

Table 7 shows the optimal hyperparameters and performance metrics of the random forest model, which varied depending on the soil property evaluated. Excellent prediction accuracy was achieved for exchangeable sodium, followed by very good performance for exchangeable calcium, magnesium, and organic matter (RPD > 2.0, R^2 > 0.76). Moderate predictions (1.4 < RPD < 2.0) were obtained for pH, electrical conductivity, calcium carbonate equivalent, available potassium, and silt content. In contrast, poor predictive performance (RPD < 1.4) was observed for the available phosphorus, exchangeable potassium, and sand and clay fractions. The optimal hyperparameters varied considerably across properties, with mtry ranging from 4 to 27, ntree from 50 to 650, and bag_fraction between 0.5 and 1.0, reflecting the different complexity and spatial structures of each soil property.

Spatial distribution of soil fertility indicators

Importance of variables

The relative importance of environmental covariates in the Random Forest models varied substantially among soil properties (Figure 2). Textural fractions (sand, silt, clay) and available phosphorus consistently exhibited low covariate importance across all predictor types, indicating limited predictability from remotely sensed and environmental variables. Conversely, chemical properties, including pH, organic matter, and exchangeable cations (Ca^{2+}, Mg^{2+}, Na^{+}) demonstrated strong associations with topographic covariates, with elevation and terrain-related variables emerging as the primary predictors. Spectral vegetation indices and synthetic aperture radar (SAR)-derived parameters contributed moderately to model performance, while Euclidean distance variables showed limited predictive value for most soil properties. Exchangeable sodium exhibited the highest sensitivity to elevation gradients, with normalized importance exceeding 35, followed by calcium and magnesium (importance > 15). This pattern suggests that soil chemical fertility is predominantly controlled by topography-mediated environmental gradients, rather than by surface spectral characteristics captured through remote sensing.

Spatial analysis of soil fertility for maize production

Figure 3 presents the spatial distribution of soil physical and chemical properties, classified according to interpretative categories (Table 1). Pronounced spatial heterogeneity was observed for most fertility indicators. Uncertainty maps are provided in Supplementary Material (Figure S1), particularly important for mobile nutrients where model performance was lower compared to stable properties.

Soil texture varied from sandy (>55% sand) in southern and western sectors to loam and

Table 7. Optimal hyperparameters and performance metrics of the RF model for predicting soil fertility properties

Element	mtry	ntree	bag_fraction	R^2	RMSE	MAE	RPD
CaCO3_eq	25	50	0.9	0.6113	4.6934	3.2783	1.6121
Ca_cmol	23	50	1	0.8218	6.6784	4.8667	2.3146
Clay	13	50	1	0.4561	7.3584	5.2027	1.2602
EC	21	100	1	0.6391	1.3660	1.0986	1.6464
K_cmol	9	100	0.9	0.3897	0.2206	0.1487	1.2833
K_disp	26	200	1	0.6620	76.7955	47.2833	1.6401
Mg_cmol	26	650	1	0.7612	0.6090	0.4610	2.0414
Na_cmol	27	500	1	0.8925	0.1258	0.0755	3.0170
OM	27	50	0.9	0.7590	0.9727	0.7567	2.0063
P_disp	4	200	1	0.3007	13.5153	8.8146	1.1574
Sand	9	600	1	0.5391	6.7598	5.5391	1.4166
Silt	26	300	1	0.6891	4.6417	3.5452	1.7589
pH	26	50	0.5	0.6940	0.1457	0.0995	1.6324

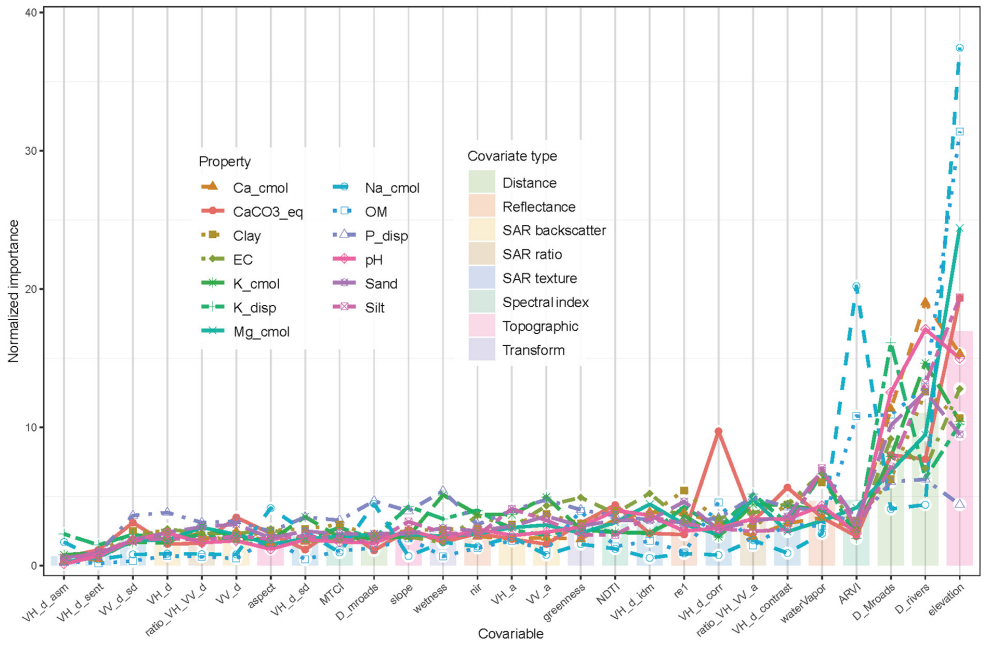

Figure 2. Environmental covariate importance in spatial prediction of soil chemical and physical properties

clay-loam (25–35% clay) in central and northern areas. Organic matter exceeded 4% in central and western zones, but was below 2% in southern and eastern sectors. Soil pH remained predominantly between 6.5 and 7.5, with values approaching 7.9 in the eastern sector. Electrical conductivity was generally low (3–9 mS/m), with localized elevated values (>9 mS/m) in northern and eastern zones, indicating incipient salinity.

Available phosphorus exceeded 15 mg/kg in northern and central areas, while southern zones showed lower availability (<10 mg/kg). Available potassium was high (>280 mg/kg) in central and eastern regions, with localized deficiencies in the southwest.

Exchangeable cations exhibited distinct patterns. Calcium and magnesium showed elevated concentrations in northeastern and central-eastern sectors. Exchangeable potassium was adequate in central areas, but decreased toward southern and western zones. Sodium exhibited localized accumulation in northeastern and eastern areas, spatially coinciding with elevated EC values. Calcium carbonate equivalent was concentrated in the eastern sector (10–20% $CaCO_3$, locally >20%), contributing to elevated pH and potential phosphorus fixation.

The co-occurrence of elevated $CaCO_3$, pH, Na, and EC in eastern sectors reflects distinct pedological conditions, possibly influenced by reduced drainage or capillary groundwater movement. These spatial patterns validate the need for site-specific nutrient management to optimize maize productivity across this heterogeneous landscape.

Spatial distribution of soil texture classes in the study area

Figure 4 shows the spatial distribution and textural classification of soils according to the USDA system (Moreno-Maroto and Alonso-Azcárate, 2022). Loam is the dominant textural class, covering most of the study area and providing favorable physical conditions for maize cultivation. Sandy clay loam and clay loam are concentrated in central and eastern sectors, offering moderate water retention but increased compaction risk.

Sandy loam and sand loam textures occur along the western and northern river corridors, reflecting fluvial sediment deposition and characterized by high drainage capacity and lower nutrient retention. Small areas of clay texture present infiltration limitations and potential waterlogging constraints in poorly drained positions.

The textural triangle confirms that most samples cluster within the loam class, with secondary concentrations in clay loam and sandy clay loam categories. This distribution reflects both heterogeneous upland parent materials and fluvial processes along river boundaries, where alluvial deposition has created texturally distinct riparian zones. Site-specific management should

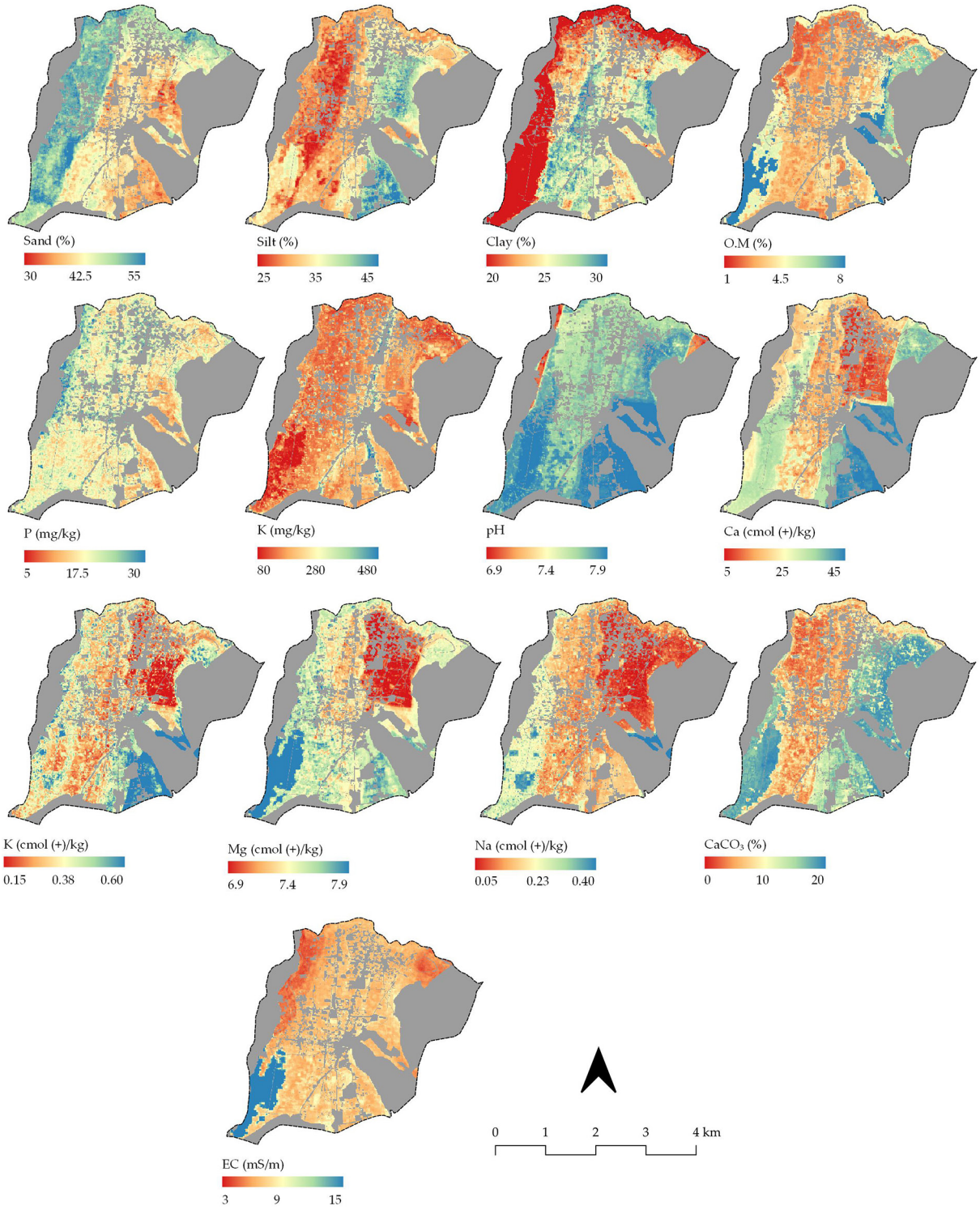

Figure 3. Spatial distribution of soil fertility parameters

account for contrasting water dynamics between well-drained fluvial areas and moisture-retentive upland zones to optimize resource use efficiency.

Spatial distribution of soil fertility levels

Figure 5 shows the spatial distribution of soil chemical suitability under three classification approaches. The Strict approach represents the most restrictive condition, as it considers only the most unfavorable variable at each site, resulting in most of the territory being classified as not suitable. This scenario highlights the most severe limitations and suggests that, without improvement interventions, agricultural use would be highly constrained.

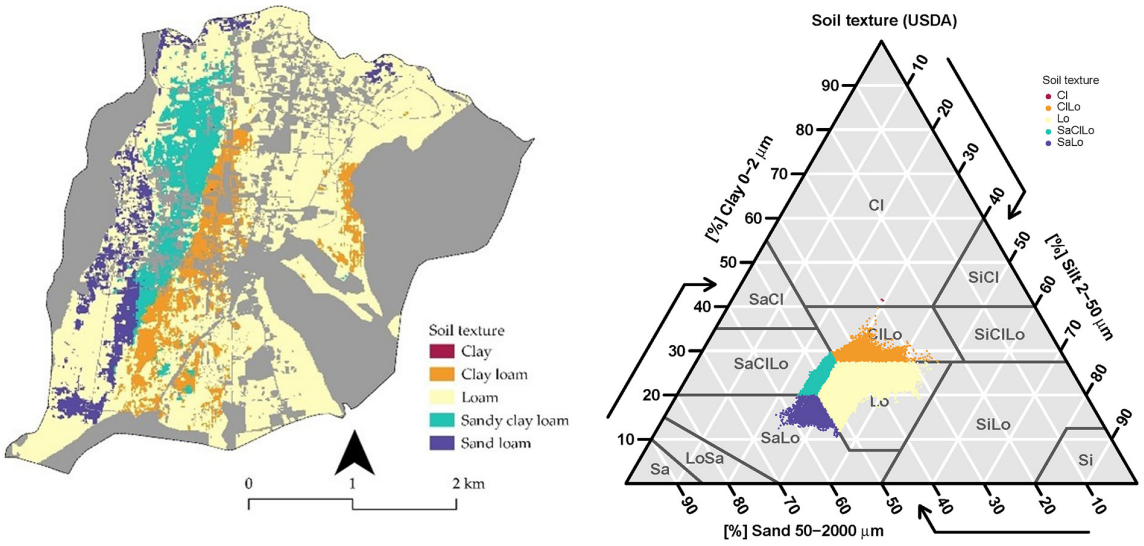

Figure 4. Spatial distribution of soil texture classes

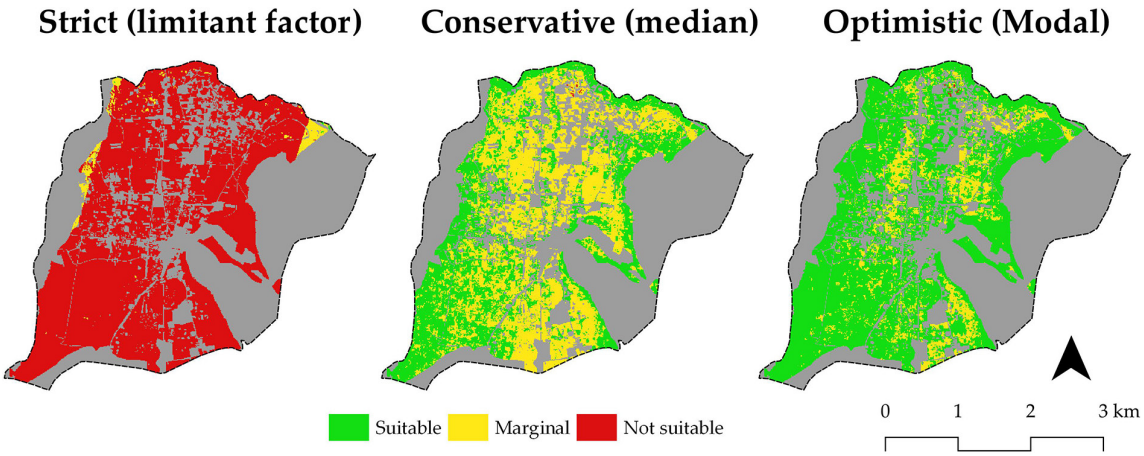

Figure 5. Spatial comparison of three classification approaches for soil chemical suitability

The Conservative approach presents a more balanced pattern, with greater spatial diversity among suitable, marginal, and unsuitable areas. This method provides an intermediate perspective of productive capacity, integrating both favorable conditions and zones with moderate limitations. Finally, the Optimistic approach assigns the largest proportion of the area as suitable, with a substantial reduction of marginal and unsuitable zones. This represents the most favorable scenario for maize cultivation, although it could overestimate the actual soil quality if restrictive factors are not carefully considered.

Fertilizer recommendations for precision management

Figure 6 shows the spatial relationship between the natural soil nutrient supply and the fertilization requirements for maize cultivation, focusing on nitrogen (N), phosphorus (P_2O_5), and potassium (K_2O). The top row illustrates the soil nutrient supply: nitrogen ranges from 9 to 60 kg/ha, with higher values in the northern and western zones; phosphorus varies between 10 and 30 kg/ha, showing central enrichment; and potassium exhibits the greatest heterogeneity (60–250 kg/ha), with elevated levels in the eastern sector. These patterns reflect strong spatial variability in the natural availability of essential nutrients for maize production.

The middle row displays the gross fertilizer requirements, calculated as the difference between crop demand and soil supply. Under this approach, nitrogen requirements range from 9 to 60 kg/ha, with critical hotspots in the southern and eastern areas; phosphorus needs vary from 0 to 10 kg/ha, mainly in the regions with low

natural supply; while potassium requirements remain minimal (0–1 kg/ha) due to adequate soil reserves. Red-colored zones indicate areas of high input dependency, where soil nutrient supply may not meet crop demands. The bottom row presents the adjusted fertilizer doses, which account for fertilizer use efficiency and nutrient partitioning into maize roots and stems. In this scenario, nitrogen adjustments range from 0 to 300 kg/ha, with high-demand patches in specific sectors; phosphorus adjustments reach up to 100 kg/ha in deficient areas, but are substantially reduced in nutrient-rich zones; and potassium remains negligible (0–1 kg/ha). Overall, the analysis highlights site-specific nutrient management patterns for maize cultivation, governed by the inverse relationship between soil nutrient supply and fertilizer requirements, with phosphorus showing the strongest spatial correlation between natural availability and reduced input demand.

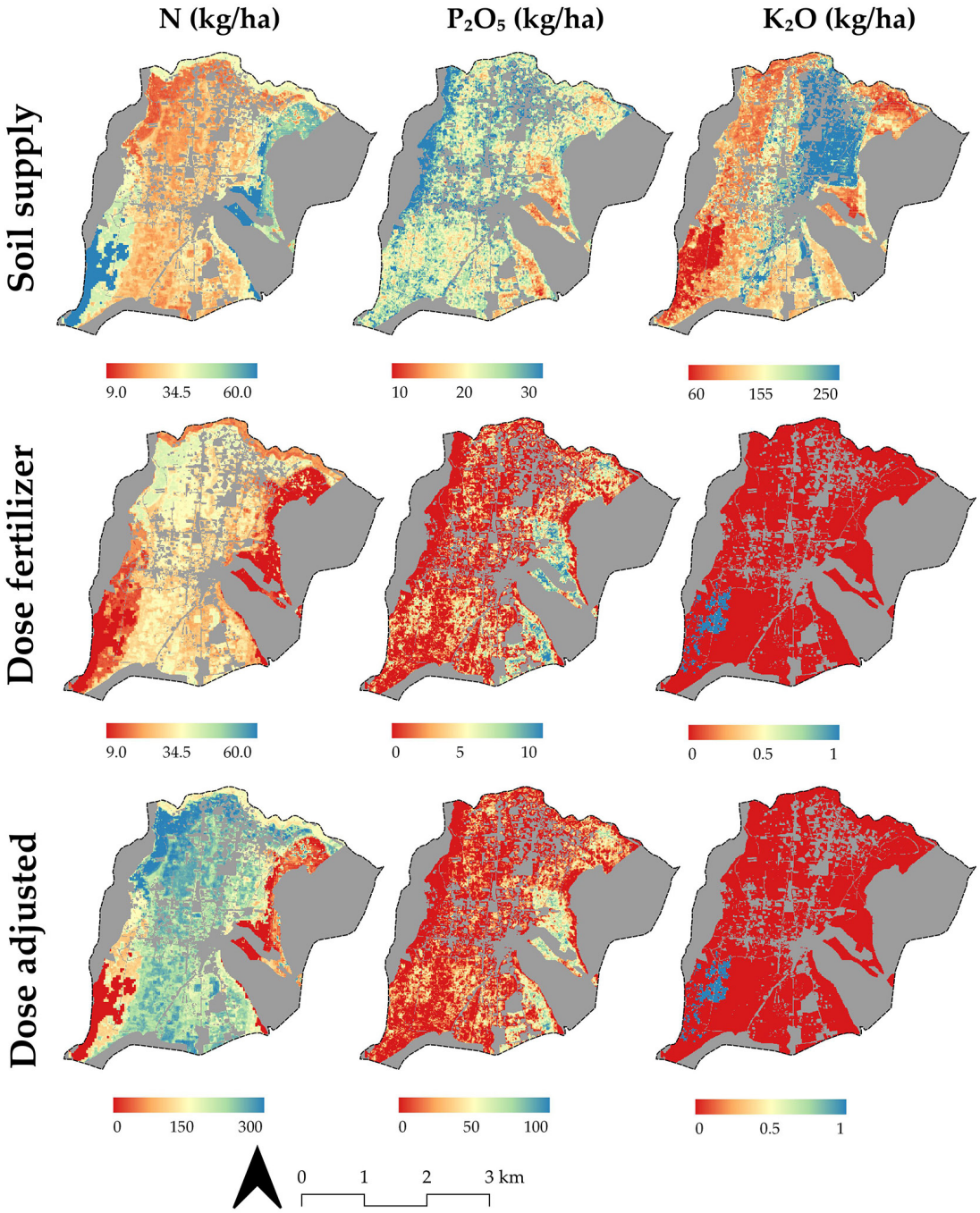

Figure 6. Spatial maps of soil nutrient supply (top row), fertilizer requirement (middle row), and adjusted nutrient dose (bottom row) for amylaceous maize. Nutrients are expressed as N, P_2O_5, and K_2O (kg/ha)

DISCUSSION

Spatial patterns of soil fertility and underlying controls

Spatial characterization revealed marked heterogeneity in soil fertility across the study area, with distinct patterns reflecting topography, parent material, and management history. Variable importance analysis (Figure 2) demonstrated that elevation and terrain-related covariates were the primary predictors of chemical properties, particularly exchangeable cations and pH (normalized importance 15–35), indicating that fertility patterns are predominantly controlled by elevation-mediated environmental gradients affecting weathering, hydrology, and nutrient redistribution (de Valença et al., 2017).

Mobile macronutrients exhibited the strongest spatial contrasts. Phosphorus showed pronounced heterogeneity, with deficiencies (<10 mg/kg) in southern zones versus adequate levels (>15 mg/kg) in northern areas, consistent with P fixation by Fe and Al oxides combined with heterogeneous fertilizer application in Andean soils (Behrends Kraemer et al., 2021; Kilic et al., 2012; Selmy et al., 2022). Potassium displayed localized deficiencies (<80 mg/kg) in southwestern areas that may compromise grain quality and stress tolerance, emphasizing the importance of K–Ca–Mg balance for crop productivity (da Silva Carneiro et al., 2022; Zhan et al., 2025).

Organic matter varied substantially (1–8%), with elevated values (>4%) in central-western zones versus depleted areas (<2%) in southern-eastern sectors, likely reflecting differential residue management across smallholder farms (Ichami et al., 2020; Sanad et al., 2024; Taghipour et al., 2025). This spatial pattern is consistent with the findings from the Junín highlands, where land-use intensification and differential management practices have resulted in substantial soil organic carbon depletion in cultivated areas compared to grasslands and less intensively managed zones (Carbajal et al., 2024; Solórzano-Acosta et al., 2025). Soil pH remained predominantly adequate (6.5–7.5) for maize, though alkaline conditions (>7.5) in eastern sectors may restrict nutrient availability (Kilic et al., 2012).

The co-occurrence of elevated pH (>7.5), EC (>9 mS/m), Na (>0.23 cmol(+)/kg), and $CaCO_3$ (10–20%) in eastern sectors suggests reduced leaching or upward capillary movement in lower topographic positions, resulting in incipient salinity and conditions that may limit P and micronutrient availability. Such patterns of carbonate accumulation in valley bottom positions have been documented in the Mantaro Valley system, where calcareous parent materials and restricted drainage promote neutral to alkaline soil conditions (Goodman-Elgar, 2008). Soil texture was predominantly loam and clay loam, favorable for maize, though sandy textures along river corridors reflect fluvial deposition creating zones with reduced water retention.

Model performance and methodological considerations

Random Forest demonstrated excellent performance ($R^2 > 0.76$, RPD > 2.0) for stable properties, including OM, pH, and exchangeable cations (Ca, Mg, Na), confirming the capacity of RFs to capture non-linear relationships between soil properties and environmental covariates (Alonso-Sarria et al., 2025; Bouslihim et al., 2024). Conversely, available P and exchangeable K showed poor predictions (R^2 = 0.30 and 0.39), reflecting complexity of their spatial distribution driven by fixation processes, leaching, and management heterogeneity (Behrends Kraemer et al.; Houben et al., 2025). These challenges in predicting mobile nutrients are particularly pronounced in smallholder farming systems, where heterogeneous management practices, localized fertilizer applications, and variable residue management create fine-scale spatial patterns that are difficult to capture with environmental covariates alone (Mponela et al., 2020; Snapp, 2022).

Textural fractions exhibited moderate accuracy for silt (R^2 = 0.69), but poor performance for sand and clay ($R^2 < 0.55$), consistent with the reports that texture, inherited from geological processes, does not respond directly to spectral covariates and is influenced by alluvial heterogeneity and surface modification (Liu et al., 2025; Mirzaeitalarposhti et al., 2022; Zhang et al., 2024). Traditional geostatistical methods like ordinary kriging effectively capture regional trends, but fail to resolve fine-scale variability critical for micro-parcel management in smallholder systems (AbdelRahman et al., 2020; Ouabo et al., 2020), validating the RF-GIS approach for precision agriculture in fragmented landscapes.

Implications for site-specific nutrient management

High-resolution fertility maps enable precise identification of zones with specific limitations, supporting site-specific fertilization that avoids over-application in balanced areas and deficiencies in critical zones (He et al., 2024; Yadav et al., 2023). The pronounced heterogeneity confirms that uniform fertilization would be economically inefficient and environmentally unsustainable.

For phosphorus, the threefold difference between deficient and adequate zones necessitates differentiated management aligned with target fertility class approaches: maintaining optimal levels through crop removal replacement, while concentrating corrective applications in deficient areas (Steinfurth et al., 2022). In highland maize systems with yields around 2 t/ha, grain P removal is approximately 5–6 kg P/ha (Haque et al., 2024), suggesting maintenance applications of 8–12 kg P/ha when accounting for typical recovery efficiencies of 40–60%. In calcareous eastern sectors (10–20% $CaCO_3$), banded placement may improve P efficiency given fixation risks.

Potassium deficiencies in southwestern areas require targeted supplementation, as critical thresholds near 150 mg/kg are established for cereal productivity (Yang et al., 2024). In highland cereal systems of Ethiopia, K application rates of 50–140 kg K/ha are recommended depending on soil K status, with critical soil K thresholds of 210 mg/kg for optimal productivity (Mulugeta et al., 2019) Adequate K–Ca–Mg balance is critical for grain quality and stress tolerance (Zhang et al., 2016).

Nitrogen management should account for OM variability (1–8%), as OM is the primary N source. Depleted areas (<2%) require higher N inputs, while elevated OM zones (>4%) may benefit from reduced rates or split applications. This aligns with the calibration strategies achieving optimal rates around 180 kg N/ha through split applications (Jia et al., 2023), and critical soil value approaches enabling 17–43% fertilizer reductions without yield loss (Yang et al., 2024).

A critical SOC threshold of 15 g C/kg (~1.5% OM) modulates fertilizer response, promoting particulate organic carbon in depleted soils versus mineral-associated organic carbon in enriched soils (Ling et al., 2025). In severely degraded soils (<2% OM), unfertilized maize achieved only 5.2 kg N/ha uptake versus 25.6 kg N/ha under fertilization (Chikowo et al., 2004), necessitating integrated organic amendments (3% biochar + 1% compost) that increased grain weight by 40%.(Abbas et al., 2024). Conversely, split N applications at 180 kg N/ha increased yields by 6.7–11.5% while reducing inputs from conventional 240 kg N/ha rates (Jia et al., 2023). Meta-analytical evidence confirms that yield responses improve with soil OM content, supporting variable-rate protocols calibrated to OM levels for optimizing productivity and efficiency(Jiang et al., 2025).

Machine learning-based recommendations in Africa increased N-use efficiency by 30% and improved wheat yields by 16–25% (Liben et al., 2024), providing precedent for potential impacts. However, adaptation to smallholder contexts requires addressing farm size, labor availability, and economic constraints. These adoption barriers reflect broader challenges documented across developing regions, where small land size, high costs, and technology-related difficulties limit precision agriculture uptake (John et al., 2023). In Sub-Saharan Africa, smallholder farmers face poor input access and unaffordable advanced methods (Onyango et al., 2021), while high Andes farmers (>2500 m) confront compounded challenges of land degradation, climate change, and limited capacity for large-scale technology adoption (Fonte et al., 2012). Structural barriers, including low educational levels with over half of Latin American farmers barely reaching basic education (Peña-Holguín et al., 2025), intersect with insufficient technical expertise and limited infrastructure. Land tenure insecurity and incomplete administration systems in Andean regions (Schling et al., 2024) suggest that successful implementation requires addressing both technological and socioeconomic dimensions simultaneously.

Study limitations and future directions

This study characterized fertility at one time point (July 2024), not capturing temporal variability in mobile nutrients influenced by seasonal rainfall and mineralization. In tropical mountain systems, nutrient availability and especially N cycling varies along elevation gradients as temperature and moisture shape pedogenesis and biogeochemical processes (Unger et al., 2010). Nitrogen mineralization is also strongly seasonal, often peaking in warmer months and varying with vegetation, elevation, and topographic position (Knoepp and Vose, 2007; Miller et al., 2009). To better predict management-sensitive properties,

integrating proximal VNIR/MIR spectroscopy with machine-learning approaches can add high-resolution information; ensembles enhanced via external parameter orthogonalization have shown gains, particularly for organic-matter–related attributes (Hutengs et al., 2024). At broader scales, including soil-forming factors can improve SOC mapping (Xia et al., 2022). Still, the benefits of adding management covariates that are context-dependent and hinge on prior knowledge of local variability and on data availability, which is often sparse in large datasets (Pusch et al., 2023).

Validation with crop yield data would strengthen recommendations and enable economic analysis. Field trials implementing differentiated management are needed to quantify responses and returns; for example, purple maize in inter-Andean Peru has shown significant yield gains and reduced N requirements when combining fertilization with *Azospirillum* inoculation, underscoring the value of response curves calibrated to local conditions (Condori et al., 2024). Practical implementation requires addressing knowledge transfer and developing the decision-support tools that fit smallholder realities lean, mobile-first, and co-designed with farmers ideally through collective approaches that spread costs and skills (Mizik, 2023).

Despite its limitations, this study delivered the first high-resolution spatial characterization of soil fertility for maize in the Mantaro Valley agroecosystem, establishing a robust baseline for tracking temporal trends and guiding site-specific management in highland systems. Critically, the mapped variability of key nutrients enables delineation of fertilization management zones and preliminary rate recommendations that can be iteratively refined with yield-response trials, seasonal resampling of mobile nutrients, and proximal sensing (VNIR/MIR) to reduce uncertainty. Coupling these maps with lightweight decision-support tools and participatory extension will improve agronomic efficiency, economic returns, and environmental performance of maize production in the valley.

CONCLUSIONS

The spatial analysis of soil fertility in maize agroecosystems of the Mantaro Valley revealed marked heterogeneity in phosphorus (P), potassium (K), organic matter (OM), and total nitrogen (N). Approximately 25% of the study area presented phosphorus deficiencies, 15% showed localized potassium shortages, and nearly 20% had organic matter levels below 2%, which directly limits nitrogen availability. In contrast, soil pH and CEC remained relatively stable across the landscape.

The integration of laboratory analyses with machine learning, particularly RF, enabled the generation of high-resolution fertility maps that captured the spatial variability of soil properties with strong predictive performance for stable variables, such as OM and exchangeable cations. These maps clearly demonstrated that uniform fertilization strategies are inefficient, since they risk nutrient surpluses in some areas and persistent deficiencies in others.

Overall, this study established a solid technical and scientific foundation for site-specific nutrient management in high-Andean maize systems. By tailoring fertilization to local soil conditions, these differentiated strategies contribute to optimizing nutrient use efficiency, sustaining maize productivity, and reducing environmental risks in the Mantaro Valley. Future research should integrate yield-response trials, seasonal monitoring of mobile nutrients, and participatory decision-support tools to refine fertilization rate recommendations as well as ensure practical adoption in smallholder contexts.

Acknowledgments

This research was funded by the INIA project "Mejoramiento de los servicios de investigación y transferencia tecnológica en el manejo y recuperación de suelos agrícolas degradados y aguas para riego en la pequeña y mediana agricultura en los departamentos de Lima, Áncash, San Martín, Cajamarca, Lambayeque, Junín, Ayacucho, Arequipa, Puno y Ucayali" CUI 2487112, of the Ministry of Agrarian Development and Irrigation (MIDAGRI) of the Peruvian Government. We would like to express our deepest gratitude to everyone who contributed to this research at the Santa Ana Experimental Station – Huancayo.

REFERENCES

1. AbdelRahman, M. A. E., Zakarya, Y. M., Metwaly, M. M., Koubouris, G. (2020). Deciphering Soil Spatial Variability through Geostatistics and Interpolation Techniques. *Sustainability*, *13*(1), 194. https://doi.org/10.3390/su13010194

2. Abdullah, H., Skidmore, A. K., Siegenthaler, A., Neinavaz, E. (2025). High-Resolution prediction of soil pH in European temperate forests using Sentinel-2 and ancillary environmental data. *Scientific Reports*, *15*(1), 28509. https://doi.org/10.1038/s41598-025-03942-4
3. Abrol, V., Sharma, P., Chary, G. R., Srinivasarao, C., Maruthi Sankar, G. R., Singh, B., Kumar, A., Hashem, A., Ibrahimova, U., Abd-Allah, E. F., Kumar, M. (2024). Integrated organic and mineral fertilizer strategies for achieving sustainable maize yield and soil quality in dry sub-humid inceptisols. *Scientific Reports*, *14*(1). https://doi.org/10.1038/s41598-024-74727-4
4. Alonso-Sarria, F., Blanco-Bernardeau, A., Gomariz-Castillo, F., Jiménez-Bastida, H., Romero-Diaz, A. (2025). Estimation of soil properties using machine learning techniques to improve hydrological modeling in a semiarid environment: Campo de Cartagena (Spain). *Earth Science Informatics*, *18*(3), 323. https://doi.org/10.1007/s12145-025-01833-w
5. Al-Shammary, A. A. G., Al-Shihmani, L. S. S., Fernández-Gálvez, J., Caballero-Calvo, A. (2024). Optimizing sustainable agriculture: A comprehensive review of agronomic practices and their impacts on soil attributes. *Journal of Environmental Management*, *364*, 121487. https://doi.org/10.1016/j.jenvman.2024.121487
6. Alvarado, R. R., Chavez, A. L. (2009). Manejo de maíz amarillo duro (Híbridos) Instituto Nacional De Innovación Agraria-Inia.
7. B Bhanukiran Reddy, Maragatham S., Santhi R, Balachandar D., Vijayalakshmi D., Davamani V., Vasu D., Gopalakrishnan M. (2024). Predictive soil mapping using random forest models: Applications in pH and soil organic matter assessment. *Plant Science Today*. https://doi.org/10.14719/pst.3865
8. Behrends Kraemer, F., Morrás, H., Fernández, P. L., Duval, M., Galantini, J., Garibaldi, L. (2021). Influence of edaphic and management factors on soils aggregates stability under no-tillage in Mollisols and Vertisols of the Pampa Region, Argentina. *Soil and Tillage Research*, *209*, 104901. https://doi.org/10.1016/j.still.2020.104901
9. Bernoux, M., Cerri, C., Arrouays, D., Jolivet, C., Volkoff, B. (1998). Bulk densities of Brazilian amazon soils related to other soil properties. *Soil Science Society of America Journal*, *62*(3), 743–749. https://doi.org/10.2136/sssaj1998.03615995006200030029x
10. Bouslihim, Y., John, K., Miftah, A., Azmi, R., Aboutayeb, R., Bouasria, A., Razouk, R., Hssaini, L. (2024). The effect of covariates on Soil Organic Matter and pH variability: a digital soil mapping approach using random forest model. *Annals of GIS*, *30*(2), 215–232. https://doi.org/10.1080/19475683.2024.2309868
11. Bravo-García, J., Camarillo-Naranjo, J. M., Blanco-Velázquez, F. J., Anaya-Romero, M. (2025). Soil organic carbon mapping through remote sensing and in situ data with random forest by using google earth engine: A case study in Southern Africa. *Land*, *14*(7), 1436. https://doi.org/10.3390/land14071436
12. Burt, R. (2004). Soil Survey Laboratory Methods Manual.
13. Butphu, S., Rasche, F., Cadisch, G., Kaewpradit, W. (2020). Eucalyptus biochar application enhances Ca uptake of upland rice, soil available P, exchangeable K, yield, and N use efficiency of sugarcane in a crop rotation system. *Journal of Plant Nutrition and Soil Science*, *183*(1), 58–68. https://doi.org/10.1002/jpln.201900171
14. Capetillo-Burela, A., López-Collado, C. J., Zetina-Lezama, R., Reynolds-Chávez, M. A., Matilde-Hernández, C., Cadena-Zapata, M., López-López, J. A. (2021). Modelo conceptual de fertilización nitrogenada para maiz (*Zea mays* L.) en Veracruz, México. *Rev. Iberoam. Bioecon. Cambio Clim.*, *7*(14), 1617–1631. https://doi.org/10.5377/ribcc.v7i14.12606
15. Chai, T., Draxler, R. R. (2014). Root mean square error (RMSE) or mean absolute error (MAE)? -Arguments against avoiding RMSE in the literature. *Geoscientific Model Development*, *7*(3), 1247–1250. https://doi.org/10.5194/gmd-7-1247-2014
16. CIMMYT. (1988). From agronomic data to farmer recommendations : an economics training manual. CIMMYT Economics Program. https://iaes.cgiar.org/sites/default/files/pdf/120.pdf?utm_source
17. Crist, E. P., Cicone, R. C. (1984). A physically-based transformation of thematic mapper data – The TM tasseled cap. *IEEE Transactions on Geoscience and Remote Sensing*, *GE-22*(3), 256–263. https://doi.org/10.1109/TGRS.1984.350619
18. da Silva Carneiro, J. S., da Costa Leite, R., Ferreira Junior, J. M., Gomes de Faria, Á. J., Godinho Silva, S. H., Clementino dos Santos, A., Ribeiro da Silva, R. (2022). Diagnosis of the spatial variability of soil nutrients and economics of precision management in degraded pastures. *Grasses*, *1*(1), 30–43. https://doi.org/10.3390/grasses1010003
19. Dawar, K., Khan, A., Mian, I. A., Khan, B., Ali, S., Ahmad, S., Szulc, P., Fahad, S., Datta, R., Hatamleh, A. A., Al-Dosary, M. A., Danish, S. (2022). Maize productivity and soil nutrients variations by the application of vermicompost and biochar. *PLOS ONE*, *17*(5), e0267483. https://doi.org/10.1371/journal.pone.0267483
20. Dharumarajan, S., Hegde, R., Singh, S. K. (2017). Spatial prediction of major soil properties using Random Forest techniques - A case study in semi-arid tropics of South India. *Geoderma Regional*, *10*, 154–162. https://doi.org/10.1016/j.geodrs.2017.07.005

21. Dobermann, A. R. (2001). Crop Potassium Nutrition – Implications For Fertilizer Recommendations. https://digitalcommons.unl.edu/agronomyfacpub
22. Fageria, N. K., Baligar, V. C. (2014). Macronutrient-use efficiency and changes in chemical properties of an oxisol as influenced by phosphorus fertilization and tropical cover crops. *Communications in Soil Science and Plant Analysis*, *45*(9), 1227–1246. https://doi.org/10.1080/00103624.2013.874030
23. FAO. (1976). *A Framework for Land Evaluation (Soils Bulletin No. 32)*. https://www.fao.org/4/x5310e/x5310e00.htm?utm_source
24. FAO. (2006a). *Plant nutrition for food security : a guide for integrated nutrient management*. Food and Agriculture Organization of the United Nations. https://www.fao.org/4/a0443e/a0443e00.pdf
25. FAO. (2006b). *Plant nutrition for food security: A guide for integrated nutrient management (FAO Fertilizer and Plant Nutrition Bulletin No. 16)*. https://www.fao.org/4/a0443e/a0443e04.pdf
26. FAO, F. A. O. of the U. N. (2006). *FAO/IAEA Agriculture & Biotechnology Laboratory*. https://www.iaea.org/sites/default/files/soilfinalweb06.pdf?utm_source
27. FAO, F. A. O. of the U. N. (2017). *GSP Guidelines for sharing national data/information to compile a Global Soil Organic Carbon (GSOC) map*. https://openknowledge.fao.org/server/api/core/bitstreams/0e9e6885-076e-4ff1-92fb-787449f11094/content?utm_source
28. FAO, F. and A. O. of the U. N. (2003). *Maize Post-harvest Operations*. https://www.fao.org/fileadmin/user_upload/inpho/docs/Post_Harvest_Compendium_-_MAIZE.pdf?utm_source
29. Garay, C. óscar, & Ochoa, A. álex. (2010). *Pronóstico Estacional de Lluvias y Temperaturas en la Cuenca del río Mantaro para su Aplicación en la Agricultura" 2007 - 2010*. https://www.igp.gob.pe/programas-de-investigacion/ciencias-de-la-atmosfera-e-hidrosfera/resources/proyectos/incagro/manual.pdf?utm_source
30. Ge, W., Zhou, J., Zheng, P., Yuan, L., Rottok, L. T. (2024). A recommendation model of rice fertilization using knowledge graph and case-based reasoning. *Computers and Electronics in Agriculture*, *219*. https://doi.org/10.1016/j.compag.2024.108751
31. Gorelick, N., Hancher, M., Dixon, M., Ilyushchenko, S., Thau, D., Moore, R. (2017). Google Earth Engine: Planetary-scale geospatial analysis for everyone. *Remote Sensing of Environment*, *202*, 18–27. https://doi.org/10.1016/j.rse.2017.06.031
32. Haralick, R. M., Shanmugam, K., Dinstein, I. (1973). Textural features for image classification. *IEEE Transactions on Systems, Man, and Cybernetics*, *SMC-3*(6), 610–621. https://doi.org/10.1109/TSMC.1973.4309314
33. Harikumaran, M., Vijayalakshmi, P. (2025). Optimizing fertilizer recommendations in precision agriculture: A novel defuzzification approach with adaptive intelligent optimization. *Knowledge-Based Systems*, *321*. https://doi.org/10.1016/j.knosys.2025.113550
34. He, Y., Bond-Lamberty, B., Myers-Pigg, A. N., Newcomer, M. E., Ladau, J., Holmquist, J. R., Brown, J. B., Falco, N. (2024). Effects of spatial variability in vegetation phenology, climate, landcover, biodiversity, topography, and soil property on soil respiration across a coastal ecosystem. *Heliyon*, *10*(9). https://doi.org/10.1016/j.heliyon.2024.e30470
35. Houben, T., Ebeling, P., Khurana, S., Schmid, J. S., Boog, J. (2025). Machine-learning based spatio-temporal prediction of soil moisture in a grassland hillslope. *Vadose Zone Journal*, *24*(2). https://doi.org/10.1002/vzj2.70011
36. Ichami, S. M., Shepherd, K. D., Hoffland, E., Karuku, G. N., Stoorvogel, J. J. (2020). Soil spatial variation to guide the development of fertilizer use recommendations for smallholder farms in western Kenya. *Geoderma Regional*, *22*. https://doi.org/10.1016/j.geodrs.2020.e00300
37. Igwe, C. A., Nkemakosi, J. T. (2007). Nutrient element contents and cation exchange capacity in fine fractions of southeastern nigerian soils in relation to their stability. *Communications in Soil Science and Plant Analysis*, *38*(9–10), 1221–1242. https://doi.org/10.1080/00103620701328347
38. INIA. (2008). *Instituto Nacional De Investigación Agraria – Inia*.
39. Ismaili, S. D. A., Moughli, L. (2014). Soil Fertility Mapping: Comparison of Three Spatial Interpolation Techniques. www.ijert.org
40. Jeon, S. H., Jang, H. J., Ng, W., Minasny, B., Kim, S. H., Shim, J. H., Roh, A., Kwon, S. ik, Yun, J. J. (2024). Predicting soil properties for fertiliser recommendation in South Korea using MIR spectroscopy. *Geoderma Regional*, *39*. https://doi.org/10.1016/j.geodrs.2024.e00901
41. Jia, Z., Zhao, S., Zhang, Q., Xia, C., Zhang, X., Zhang, Y., Gao, Q. (2023). Multi-stage fertilizer recommendation for spring maize at the field scale based on narrowband vegetation indices. *Computers and Electronics in Agriculture*, *213*. https://doi.org/10.1016/j.compag.2023.108236
42. Julca-Otiniano, A., Meneses-Florián, L., Blas-Sevillano, R., Bello-Amez, S. (2006). La materia orgánica, importancia y experiencia de su uso en la agricultura. *Idesia (Arica)*, *24*(1). https://doi.org/10.4067/S0718-34292006000100009
43. Kilic, K., Kilic, S., Kocyigit, R. (2012). Assessment of spatial variability of soil properties in areas under different land use732 Agricultural Academy. In *Bulgarian Journal of Agricultural Science 18*(5).

44. Kuunya, R., Mustafa Ahmed Osman, M., Ragán, P. (2025). Soil, nutrient, and fertiliser requirements for maize (*Zea mays*) production: A narrative review. *Acta Agraria Debreceniensis*, *1*, 85–97. https://doi.org/10.34101/actaagrar/1/15223
45. Li, H., Van den Bulcke, J., Mendoza, O., Deroo, H., Haesaert, G., Dewitte, K., De Neve, S., Sleutel, S. (2022). Soil texture controls added organic matter mineralization by regulating soil moisture – evidence from a field experiment in a maritime climate. *Geoderma*, *410*, 115690. https://doi.org/10.1016/j.geoderma.2021.115690
46. Liaw, A., Wiener, M. (2002). Classification and Regression by random Forest (Vol. 2, Issue 3). http://www.stat.berkeley.edu/
47. Liben, F., Abera, W., Chernet, M. T., Ebrahim, M., Tilaye, A., Erkossa, T., Degefie, D. T., Mponela, P., Kihara, J., Tamene, L. (2024). Site-specific fertilizer recommendation using data driven machine learning enhanced wheat productivity and resource use efficiency. *Field Crops Research*, *313*. https://doi.org/10.1016/j.fcr.2024.109413
48. Liu, H., Yang, J., He, P., Bai, Y., Jin, J., Drury, C. F., Zhu, Y., Yang, X., Li, W., Xie, J., Yang, J., Hoogenboom, G. (2012). Optimizing parameters of CSM-CERES-maize model to improve simulation performance of maize growth and nitrogen uptake in Northeast China. *Journal of Integrative Agriculture*, *11*(11), 1898–1913. https://doi.org/10.1016/S2095-3119(12)60196-8
49. Liu, J., Ye, Y., Wang, C., Chen, S., Jiang, Y., Guo, X., Jiang, Y. (2025). Machine learning-based comparative analysis on direct and indirect mapping of soil texture types through soil particle size fractions using multi-source remote sensing. *Agriculture*, *15*(13), 1395. https://doi.org/10.3390/agriculture15131395
50. Ma, G., Ding, J., Han, L., Zhang, Z., Ran, S. (2021). Digital mapping of soil salinization based on Sentinel-1 and Sentinel-2 data combined with machine learning algorithms. *Regional Sustainability*, *2*(2), 177–188. https://doi.org/10.1016/j.regsus.2021.06.001
51. MacCarthy, D. S., Adamtey, N., Freduah, B. S., Fosu-Mensah, B. Y., Ofosu-Budu, G. K., Fliessbach, A. (2023). Modeling the effect of soil fertility management options on maize yield stability under variable climate in a sub-humid zone in Ghana. *Frontiers in Sustainable Food Systems*, *7*. https://doi.org/10.3389/fsufs.2023.1132732
52. Maiti, D., Das, D. K., Pathak, H. (2006). Simulation of fertilizer requirement for irrigated wheat in Eastern India using the QUEFTS model. *The Scientific World JOURNAL*, *6*, 231–245. https://doi.org/10.1100/tsw.2006.43
53. McBratney, A. B., Mendonça Santos, M. L., Minasny, B. (2003). On digital soil mapping. *Geoderma*, *117*(1–2), 3–52. https://doi.org/10.1016/S0016-7061(03)00223-4
54. Mcfarland, M. L., Haby, V. A., Redmon, L. A., Bade, D. H. (2001). *Managing Soil Acidity What Causes Soil Acidity?*
55. MIDAGRI. (2019). *Requerimientos Agroclimáticos del cultivo de Maíz Choclo*. www.minagri.gob.pe
56. MIDAGRI. (2020). *Manual Tecnico del Cultivo de maiz*.
57. MIDAGRI, M. de D. A. y R. (2009). Plan estrategico sectorial regional agrario 2009–*2015*. https://www.midagri.gob.pe/portal/download/pdf/conocenos/transparencia/planes_estrategicos_regionales/junin.pdf
58. Mirzaeitalarposhti, R., Shafizadeh-Moghadam, H., Taghizadeh-Mehrjardi, R., Demyan, M. S. (2022). Digital soil texture mapping and spatial transferability of machine learning models using Sentinel-1, Sentinel-2, and terrain-derived covariates. *Remote Sensing*, *14*(23), 5909. https://doi.org/10.3390/rs14235909
59. Moreno-Maroto, J. M., Alonso-Azcárate, J. (2022). Evaluation of the USDA soil texture triangle through Atterberg limits and an alternative classification system. *Applied Clay Science*, *229*, 106689. https://doi.org/10.1016/j.clay.2022.106689
60. Mouazen, A. M., Shi, Z. (2021). Estimation and mapping of soil properties based on multi-source data fusion. *Remote Sensing*, *13*(5), 978. https://doi.org/10.3390/rs13050978
61. Ingle, S. N., Nagaraju, M. S. S., Sahu, N., Srivastava, R., Tiwary, P., Sen, T. K., Nasre, R. A. (2018). Mapping of spatial variability in soil properties and soil fertility for site-specific nutrient management in Bareli Watershed, Seoni District of Madhya Pradesh Using Geostatistics and GIS. *International Journal of Current Microbiology and Applied Sciences*, *7*(10), 2299–2306. https://doi.org/10.20546/ijcmas.2018.710.266
62. NOM-021-RECNAT-2000. (2002). *NORMA Oficial Mexicana NOM-021-RECNAT-2000, Que establece las especificaciones de fertilidad, salinidad y clasificación de suelos. Estudios, muestreo y análisis.*
63. Nwite, J. N., Ajana, A. J., Alinchi, I. (2022). Effect of pH on soil chemical properties and maize performance in Abakaliki, Nigeria. *Agricultural Science Digest - A Research Journal*, *Of*. https://doi.org/10.18805/ag.DF-409
64. Ouabo, R. E., Sangodoyin, A. Y., Ogundiran, M. B. (2020). Assessment of ordinary kriging and inverse distance weighting methods for modeling chromium and cadmium soil pollution in e-waste sites in Douala, Cameroon. *Journal of Health and Pollution*, *10*(26). https://doi.org/10.5696/2156-9614-10.26.200605
65. Pebesma, E. (2018). Simple Features for R: Standardized Support for Spatial Vector Data. *The R Journal*, *10*(1), 439. https://doi.org/10.32614/RJ-2018-009

66. Phinzi, K., Bertalan, L., Chakilu, G. G., Szabó, S. (2025). Improving the spatial prediction of topsoil properties in a typical grazing area using multi-season PlanetScope spectral covariates and data mining techniques. *Earth Science Informatics*, *18*(2), 222. https://doi.org/10.1007/s12145-025-01748-6

67. Pizarro, S., Requena-Rojas, E., Barboza, E., Peña-Elme, E., Arias-Arredondo, A., Ccopi, D. (2025). Ecological and carcinogenic risk assessment of potentially toxic elements in rangelands and croplands around Lake Junin (Peru): Integrating remote sensing, machine learning, and land cover segmentation. *Science of The Total Environment*, *999*, 180327. https://doi.org/10.1016/j.scitotenv.2025.180327

68. QGIS Development Team. (2024). *QGIS Development Team. (2024). QGIS Geographic Information System (Versión 3.36). Open Source Geospatial Foundation.* https://qgis.org

69. R Core Team. (2024). *R: A* language and environment for statistical computing (Version 4.x. R Foundation for Statistical Computing). https://www.r-project.org/

70. Randhawa, M. K., Dhaliwal, S. S., Sharma, V., Toor, A. S., Sharma, S., Kaur, M., Verma, G. (2021). Nutrient use efficiency as a strong indicator of nutritional security and builders of soil nutrient status through integrated nutrient management technology in a rice-wheat system in Northwestern India. *Sustainability*, *13*(8), 4551. https://doi.org/10.3390/su13084551

71. Rangaiah, K. M., Nagaraju, B., Shankaraiah, S. K., Kasturappa, G., Kadappa, B. P., Sugatur Narayanaswamy, U. K., Saqeebulla, M., Dey, P. (2024). Enhancing yield, uptake and nutrient use efficiency of brinjal through soil test crop response approach. *Communications in Soil Science and Plant Analysis*, *55*(7), 998–1014. https://doi.org/10.1080/00103624.2023.2289988

72. Rao, S., Meunier, F., Ehosioke, S., Lesparre, N., Kemna, A., Nguyen, F., Garré, S., Javaux, M. (2019). Impact of maize roots on soil–root electrical conductivity: A simulation study. *Vadose Zone Journal*, *18*(1). https://doi.org/10.2136/vzj2019.04.0037

73. Rashmi, I., Shirale, A., Kartikha, K. S., Shinogi, K. C., Meena, B. P., Kala, S. (2017). Leaching of Plant Nutrients from Agricultural Lands. In *Essential Plant Nutrients* (pp. 465–489). Springer International Publishing. https://doi.org/10.1007/978-3-319-58841-4_19

74. Raun, W. R., Johnson, G. V. (1999). Improving nitrogen use efficiency for cereal production. *Agronomy Journal*, *91*(3), 357–363. https://doi.org/10.2134/agronj1999.00021962009100030001x

75. Saidi, D. (2012). Relationship between cation exchange capacity and the saline phase of Cheliff sol. *Agricultural Sciences*, *3*(3), 434–443. https://doi.org/10.4236/as.2012.33051

76. Sanad, H., Moussadek, R., Mouhir, L., Oueld Lhaj, M., Dakak, H., El Azhari, H., Yachou, H., Ghanimi, A., Zouahri, A. (2024). Assessment of soil spatial variability in agricultural ecosystems using multivariate analysis, soil quality index (SQI), and geostatistical approach: A case study of the Mnasra Region, Gharb Plain, Morocco. *Agronomy*, *14*(6). https://doi.org/10.3390/agronomy14061112

77. Selmy, S., El-Aziz, S. A., El-Desoky, A., El-Sayed, M. (2022). Characterizing, predicting, and mapping of soil spatial variability in Gharb El-Mawhoub area of Dakhla Oasis using geostatistics and GIS approaches. *Journal of the Saudi Society of Agricultural Sciences*, *21*(6), 383–396. https://doi.org/10.1016/j.jssas.2021.10.013

78. Senamhi, S. N. de M. e H. (2020). Climas del Perú Mapa de Cllasificación Climática Nacional. In *Ministerio del Ambiente 53*(9).

79. Shahare, Y. R., Singh, M. P., Singh, S. P., Singh, P., Diwakar, M. (2024). ASUR: Agriculture soil fertility assessment using random forest classifier and regressor. *Procedia Computer Science*, *235*, 1732–1741. https://doi.org/10.1016/j.procs.2024.04.164

80. Sharma, P., Leigh, L., Chang, J., Maimaitijiang, M., Caffé, M. (2022). Above-ground biomass estimation in oats using UAV remote sensing and machine learning. *Sensors*, *22*(2). https://doi.org/10.3390/s22020601

81. Smil, V. (1999). Nitrogen in crop production: An account of global flows. *Global Biogeochemical Cycles*, *13*(2), 647–662. https://doi.org/10.1029/1999GB900015

82. Steinfurth, K., Börjesson, G., Denoroy, P., Eichler-Löbermann, B., Gans, W., Heyn, J., Hirte, J., Huyghebaert, B., Jouany, C., Koch, D., Merbach, I., Mokry, M., Mollier, A., Morel, C., Panten, K., Peiter, E., Poulton, P. R., Reitz, T., Rubæk, G. H., … Buczko, U. (2022). Thresholds of target phosphorus fertility classes in European fertilizer recommendations in relation to critical soil test phosphorus values derived from the analysis of 55 European long-term field experiments. *Agriculture, Ecosystems and Environment*, *332*. https://doi.org/10.1016/j.agee.2022.107926

83. Taghipour, F., Emadi, S. M., Danesh, M., Ghajar Sepanlou, M. (2025). Interpolation and artificial neural network to estimate soil spatial variability affected by land use and altitude. *Journal of South American Earth Sciences*, *157*. https://doi.org/10.1016/j.jsames.2025.105485

84. Tamburi, V., Shetty, A., Shrihari, S. (2021). Spatial variability of vertisols nutrients in the Deccan plateau region of north Karnataka, India. *Environment, Development and Sustainability*, *23*(2), 2910–2923. https://doi.org/10.1007/s10668-020-00700-6

85. Tennekes, M. (2018). tmap : Thematic Maps in *R*. *Journal of Statistical Software*, *84*(6). https://doi.org/10.18637/jss.v084.i06

86. Tikuye, B. G., Ray, R. L. (2025). Predicting future corn suitability zones under climate change scenarios

in the United States of America. *Journal of Agriculture and Food Research*, *22*, 102129. https://doi.org/10.1016/J.JAFR.2025.102129

87. Tola, D., Satgé, F., Pillco Zolá, R., Sainz, H., Condori, B., Miranda, R., Yujra, E., Molina-Carpio, J., Hostache, R., Espinoza-Villar, R. (2024). soil salinity mapping of plowed agriculture lands combining radar Sentinel-1 and optical Sentinel-2 with topographic data in machine learning models. *Remote Sensing*, *16*(18), 3456. https://doi.org/10.3390/rs16183456
88. ul Shahid, Z., Ali, M., Shahzad, K., Danish, S., Alharbi, S. A., Ansari, M. J. (2023). Enhancing maize productivity by mitigating alkaline soil challenges through acidified biochar and wastewater irrigation. *Scientific Reports*, *13*(1), 20800. https://doi.org/10.1038/s41598-023-48163-9
89. Urbina-Salazar, D., Vaudour, E., Richer-de-Forges, A. C., Chen, S., Martelet, G., Baghdadi, N., Arrouays, D. (2023). Sentinel-2 and Sentinel-1 bare soil temporal mosaics of 6-year periods for soil organic carbon content mapping in Central France. *Remote Sensing*, *15*(9), 2410. https://doi.org/10.3390/rs15092410
90. Urso, L., Petermann, E., Gnädinger, F., Hartmann, P. (2023). Use of random forest algorithm for predictive modelling of transfer factor soil-plant for radiocaesium: A feasibility study. *Journal of Environmental Radioactivity*, *270*, 107309. https://doi.org/10.1016/j.jenvrad.2023.107309
91. Valera A. R. V, Rodríguez, E. R. A. (2023). Spatial analysis of soil fertility using geostatistical techniques and artificial neural networks. *Qeios*. https://doi.org/10.32388/0jafr0
92. Vasquez-Zambrano, E., Woittiez, L. S., van Heerwaarden, J., Rusinamhodzi, L., Hauser, S., Giller, K. E. (2025). Deriving fertiliser recommendations for cocoa: An offtake model approach. *European Journal of Agronomy*, *164*. https://doi.org/10.1016/j.eja.2024.127463
93. Wang, D., Li, Z., Wang, Q. (2024). Estimation of mercury uptake and distinction of corn cultivation in China. *Science of The Total Environment*, *906*, 167508. https://doi.org/10.1016/J.SCITOTENV.2023.167508
94. Wickham, H., Averick, M., Bryan, J., Chang, W., McGowan, L., François, R., Grolemund, G., Hayes, A., Henry, L., Hester, J., Kuhn, M., Pedersen, T., Miller, E., Bache, S., Müller, K., Ooms, J., Robinson, D., Seidel, D., Spinu, V., … Yutani, H. (2019). Welcome to the Tidyverse. *Journal of Open Source Software*, *4*(43), 1686. https://doi.org/10.21105/joss.01686
95. Yadav, T. C., Singh, Y. P., Yadav, S. S., Singh, A., Subhash, Patle, T. (2023). Spatial variability in soil properties, delineation site-specific management division based on soil fertility using fuzzy clustering in Gwalior, Madhya Pradesh, India. *International Journal of Plant & Soil Science*, *35*(6), 49–78. https://doi.org/10.9734/ijpss/2023/v35i62840
96. Yang, W., Yu, J., Li, Y., Jia, B., Jiang, L., Yuan, A., Ma, Y., Huang, M., Cao, H., Liu, J., Qiu, W., Wang, Z. (2024). Optimized NPK fertilizer recommendations based on topsoil available nutrient criteria for wheat in drylands of China. *Journal of Integrative Agriculture*, *23*(7), 2421–2433. https://doi.org/10.1016/j.jia.2023.11.049
97. Yermiyahu, U., Zipori, I., Faingold, I., Yusopov, L., Faust, N., Bar-Tal, A. (2017). Polyhalite as a multi nutrient fertilizer – potassium, magnesium, calcium and sulfate. *Israel Journal of Plant Sciences*, *64*(3–4), 145–157. https://doi.org/10.1163/22238980-06401001
98. Zambrano, J. L., Yánez, C. F., Sangoquiza, C. A. (2021). Maize breeding in the highlands of Ecuador, Peru, and Bolivia: A review. *Agronomy*, *11*(2), 212. https://doi.org/10.3390/agronomy11020212
99. Zhan, D., Liu, Y., Yang, W., Lu, M., Song, Y. (2025). Spatial variability of soil salinity in coastal saline-alkali farmlands: A novel approach integrating a stacked model with the reconstructed in-situ hyperspectral feature. *Computers and Electronics in Agriculture*, *235*. https://doi.org/10.1016/j.compag.2025.110376
100. Zhang, B., Zhang, B., Xu, Y., Yan, X., Wang, S., Yang, X., Yang, H., Zhang, G., Zhang, W., Chen, T., Liu, G. (2024). Shift in potential pathogenic bacteria during permafrost degradation on the Qinghai-Tibet Plateau. *Science of The Total Environment*, *954*, 176778. https://doi.org/10.1016/j.scitotenv.2024.176778
101. Zhang, G., Wang, X., Sun, B., Zhao, H., Lu, F., Zhang, L. (2016). Status of mineral nitrogen fertilization and net mitigation potential of the state fertilization recommendation in Chinese cropland. *Agricultural Systems*, *146*, 1–10. https://doi.org/10.1016/j.agsy.2016.03.012
102. Zhang, W. chun, Zhang, X., Wu, W., Liu, H. bin. (2024). The spatial variability of temporal changes in soil organic carbon and its drivers in a mountainous agricultural region of China. *Catena*, *246*. https://doi.org/10.1016/j.catena.2024.108402
103. Zhou, Q., Lyu, D., Li, W., Wen, Y., Wang, Z. (2024). Effects of irrigation amount and salinity levels on maize (*Zea mays* L.) growth, water productivity and carbon emissions in arid region of Northwest China. *Agronomy*, *14*(11), 2656. https://doi.org/10.3390/agronomy14112656